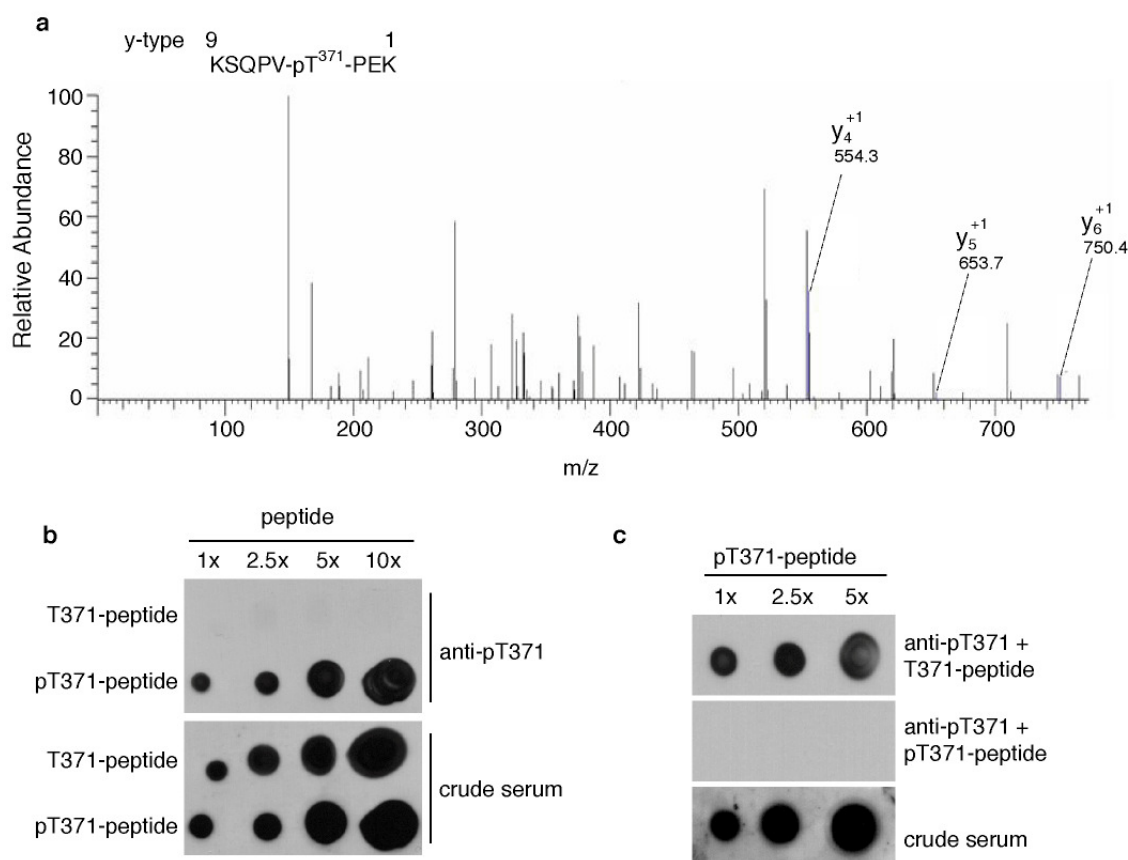
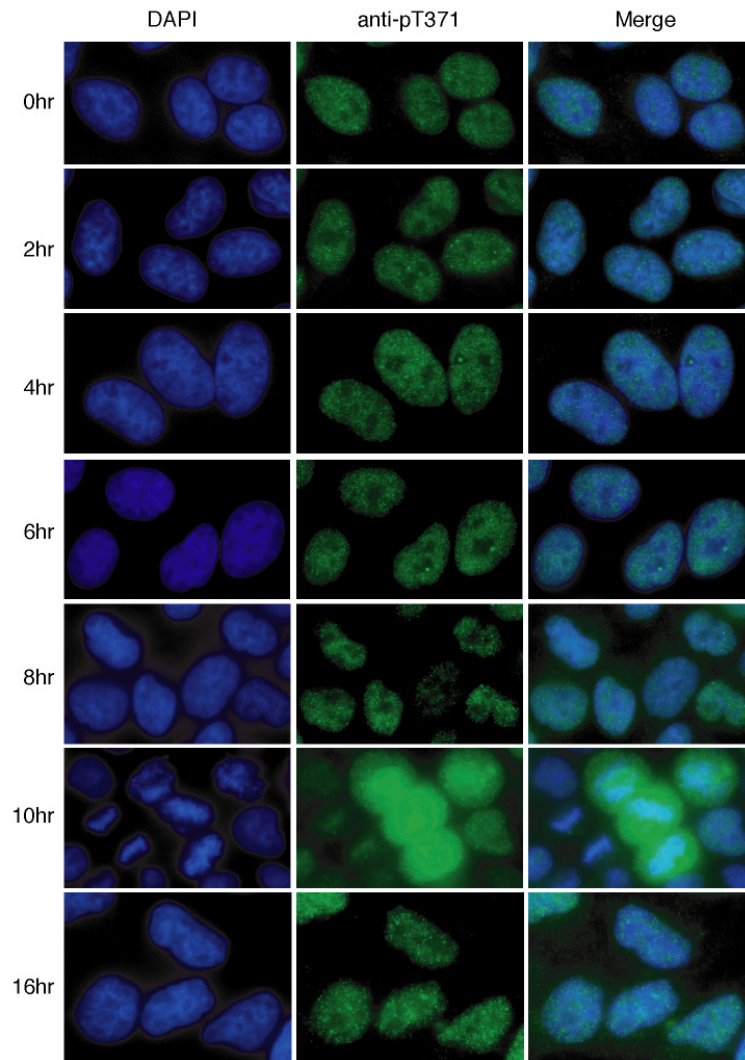


## Supplementary Figure S1 McKerlie &amp; Zhu



**Supplementary Figure. S1.** T371 of TRF1 is phosphorylated *in vivo*. **(a)** LC/MS/MS analysis was performed on TRF1 immunoprecipitated from HT1080 cells. The spectrum of the peptide identified to contain phosphorylated threonine at position 371 is shown with the relative abundance plotted against the monoisotopic mass (*m/z*). The *m/z* peaks from the y-type ions are indicated. Mass spectrometry analysis of Flag-tagged TRF1 was done through service provided by WEMB Biochem. Inc., Toronto, Canada (<http://www.wembbiochem.com/>). **(b)** Affinity-purified anti-pT371 antibody specifically recognizes TRF1 peptide containing phosphorylated T371 (pT371-peptide). An increasing amount of peptide either carrying unmodified T371 (T371-peptide) or phosphorylated T371 (pT371-peptide) was spotted on a nitrocellulose membrane, followed by immunoblotting with affinity-purified anti-pT371 antibody or crude serum. The amount of peptide spotted from left to right is 0.7  $\mu\text{g}$ , 1.75  $\mu\text{g}$ , 3.5  $\mu\text{g}$  and 7  $\mu\text{g}$ . **(c)** Peptide competition assays. Affinity-purified anti-pT371 antibody was incubated with 5.5  $\mu\text{g}$  of either unmodified (T371-peptide) or phosphorylated peptide (pT371-peptide) prior to immunoblotting. Crude serum was used to show the presence of pT371-peptide on the nitrocellulose membrane. The amount of pT371-peptide spotted from left to right is 0.7  $\mu\text{g}$ , 1.75  $\mu\text{g}$  and 3.5  $\mu\text{g}$ .

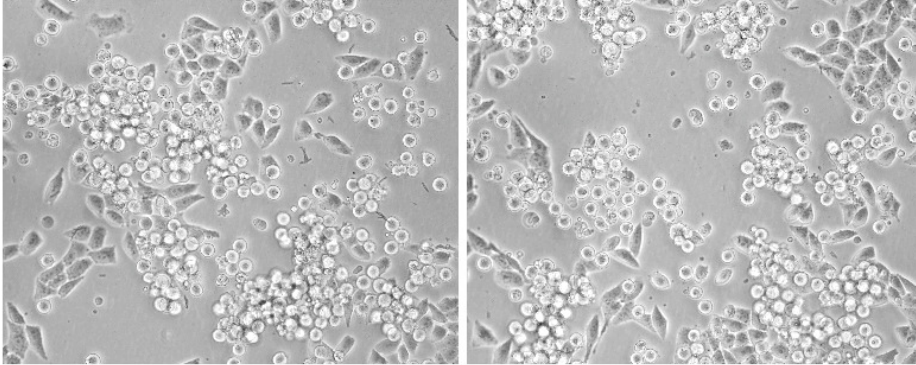
## Supplementary Figure S2 McKerlie &amp; Zhu



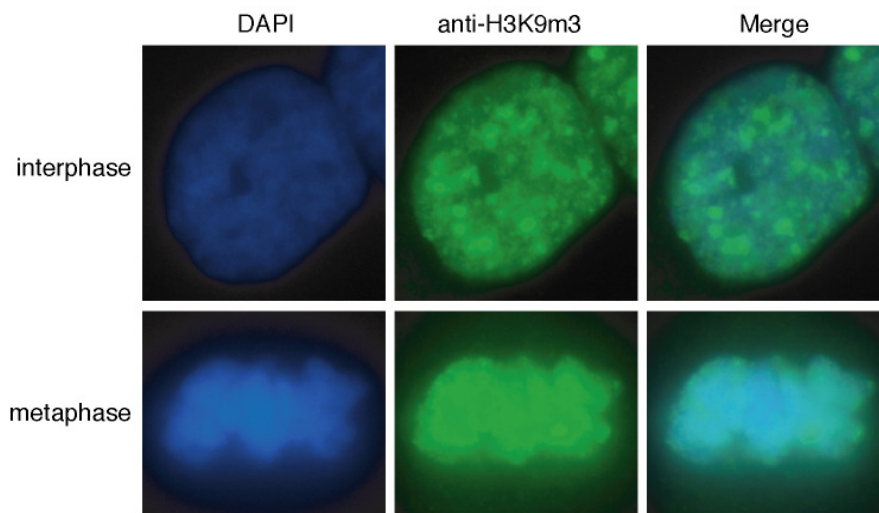
**Supplementary Figure S2.** Phosphorylation of T371 of TRF1 is specifically up regulated in mitosis. Indirect immunofluorescence using anti-pT371 antibody was performed on HeLaI.2.11 cells released for 0-16 h from a double thymidine block. Cell nuclei were stained with DAPI, shown in blue.

## Supplementary Figure S3 McKerlie &amp; Zhu

a



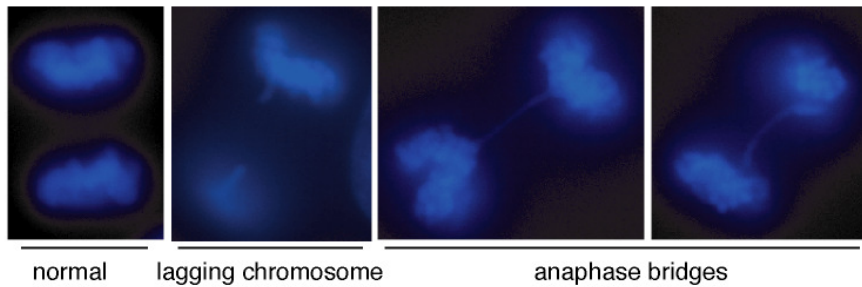
b



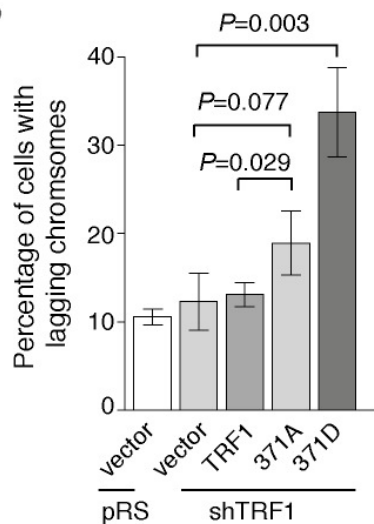
**Supplementary Figure S3.** Analysis of nocodazole treatment and chromatin association of the heterochromatic mark H3K9m3 in mitosis. **(a)** Live cell images were taken for HeLaI.2.11 cells that had been treated with nocodazole for 16 hr. **(b)** Indirect immunofluorescence using anti-H3K9m3 antibody was performed on HeLaI.2.11 cells. Cell nuclei were stained with DAPI shown in blue.

## Supplementary Figure S4 McKerlie &amp; Zhu

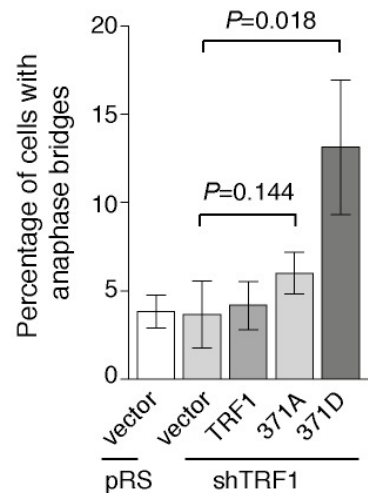
a



b

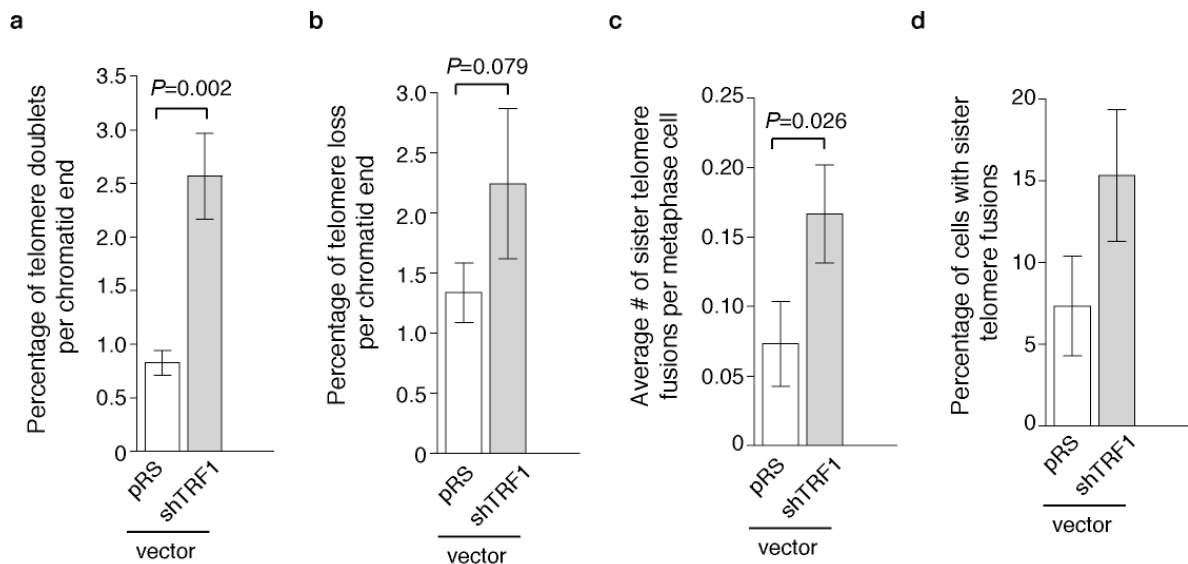


c



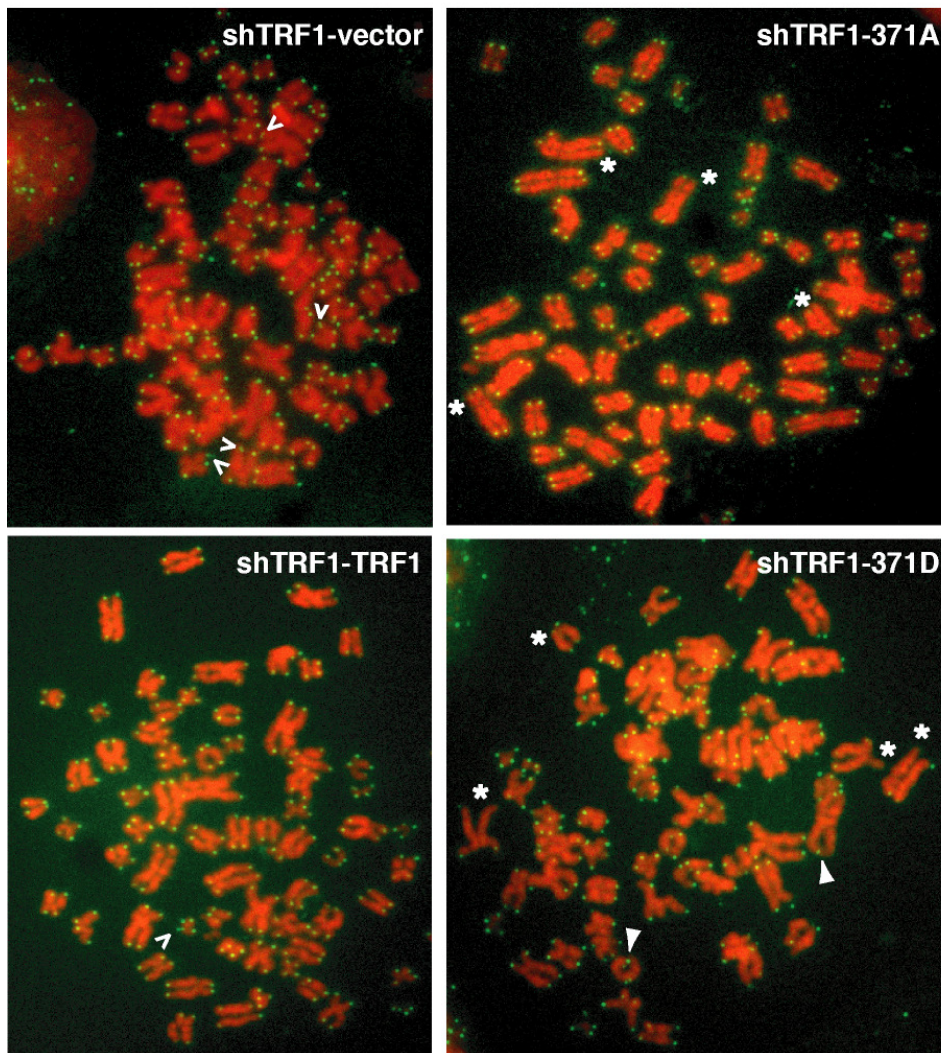
**Supplementary Figure S4.** Occurrence of lagging chromosomes and anaphase bridges in TRF1-depleted HeLaII cells expressing various TRF1 alleles. **(a)** Images of cells either normal or carrying lagging chromosomes or anaphase bridges. TRF1-depleted HeLaII cells expressing various constructs were fixed and stained directly with DAPI. Anaphase cells were inspected for the presence of lagging chromosomes or anaphase bridges. **(b)** & **(c)** Percentage of anaphase cells bearing lagging chromosomes and anaphase bridges respectively. Scoring of each cell line was done in a blind manner. A total of 300 anaphase cells from each of three independent experiments were scored. Standard deviations derived from three independent experiments are indicated.

## Supplementary Figure S5 McKerlie &amp; Zhu

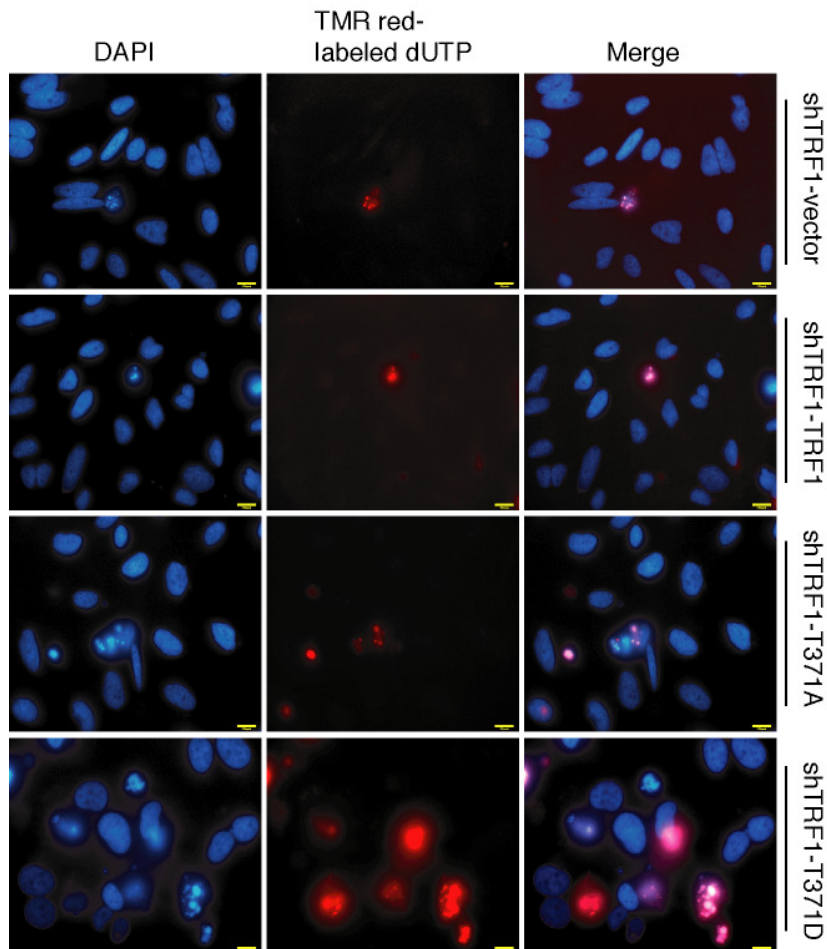


**Supplementary Figure S5.** Depletion of TRF1 leads to an accumulation of telomere doublets, telomere loss and sister telomere fusions. **(a-d)** Quantification of telomere abnormalities in HeLaII cells stably expressing either shTRF1/vector pWZL-N-myc or pRS/vector pWZL-N-myc. pWZL-N-myc is the vector used to express various Myc-tagged TRF1 proteins. For each cell line, a total of 69-71 metaphase cells were scored. Standard deviations derived from three independent experiments are indicated.

Supplementary Figure S6 McKerlie &amp; Zhu

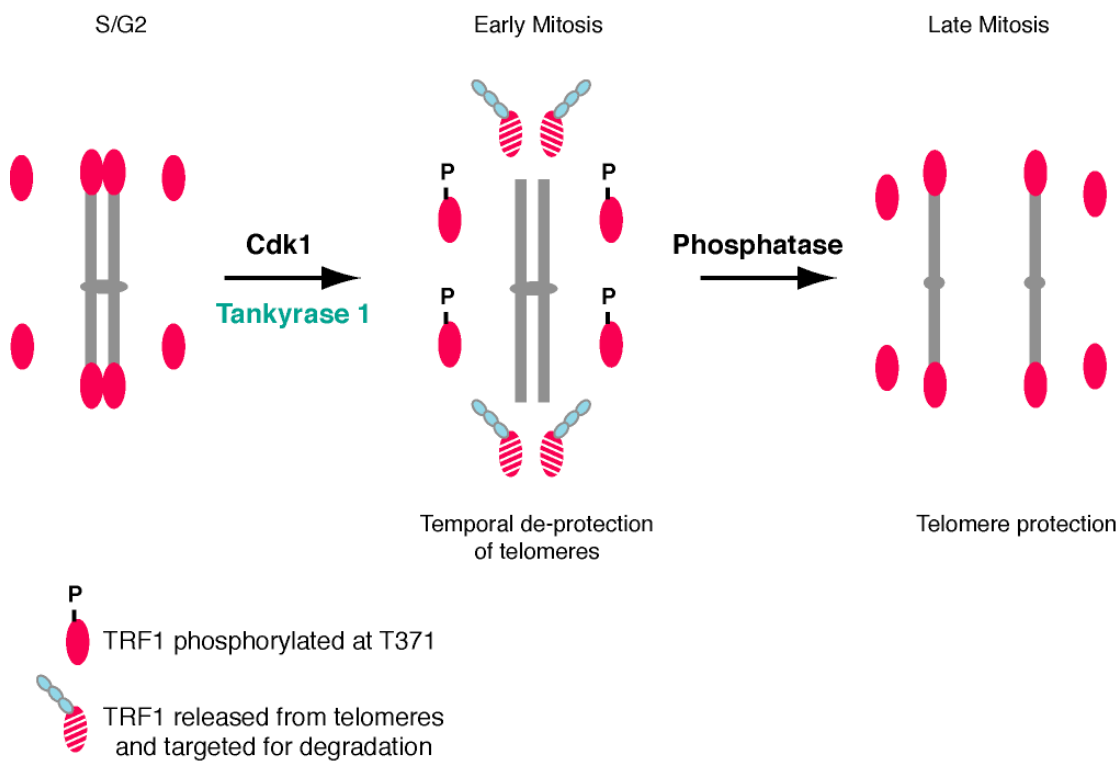


**Supplementary Figure S6.** Amino acid substitutions at position T371 of TRF1 induce telomere instability. Metaphase spreads of TRF1-depleted HeLaII cells expressing various constructs as indicated. Metaphase chromosomes were stained with DAPI and false-colored in red. Telomeric DNA was detected by FISH using a FITC-conjugated (CCCTAA)<sub>3</sub>-containing PNA probe in green. Open arrows: telomere doublets. Asterisks represent telomere loss whereas filled arrows indicate sister telomere fusions.

**Supplementary Figure S7 McKerlie & Zhu**

**Supplementary Figure S7.** TUNEL assay. TRF1-depleted HeLaII cells expressing various constructs as indicated were stained with TMR-red, which distinguishes apoptotic cells, and counterstained with DAPI in blue.

## Supplementary Figure S8 McKerlie &amp; Zhu



**Supplementary Figure S8.** Model for the role of Cdk1 in controlling the resolution of sister telomeres. We propose that upon entry into mitosis, Cdk1 phosphorylates unbound TRF1 at T371 and this phosphorylation sequesters it from associating with telomeres. Such phosphorylation, perhaps in conjunction with the action of tankyrase 1, results in a net loss of TRF1 from telomeres, promoting the temporal de-protection of telomeres as well as the resolution of sister telomeres. In late mitosis, TRF1 undergoes dephosphorylation at T371 and this dephosphorylation allows re-association of TRF1 with telomeres and re-establishment of telomere protection.